Effects of internal noise for rate oscillations during CO oxidation on platinum surfaces

Cite as: J. Chem. Phys. **122**, 134708 (2005); https://doi.org/10.1063/1.1874933
Submitted: 03 June 2004 . Accepted: 12 January 2005 . Published Online: 04 April 2005

Zhonghuai Hou, Ting Rao, and Houwen Xin

Effects of internal noise for rate oscillations during CO oxidation on platinum surfaces

Zhonghuai Hou,[a] Ting Rao, and Houwen Xin
Department of Chemical Physics, University of Science and Technology of China, Hefei, Anhui 230026, People's Republic of China

(Received 3 June 2004; accepted 12 January 2005; published online 4 April 2005)

We have studied the influence of internal noise on the reaction rate oscillation during carbon-monoxide oxidation on single crystal platinum surfaces using chemical Langevin equations. Considering that the surface is divided into small well-mixed cells, we have focused on the dynamic behavior inside a single cell. Internal noise can induce rate oscillations and the performance of the stochastic rate oscillations shows double maxima with the variation of the internal noise intensity, demonstrating the occurrence of internal noise coherent biresonance. The relationship between such a phenomenon with the deterministic bifurcation features of the system is also discussed. © *2005 American Institute of Physics*. [DOI: 10.1063/1.1874933]

I. INTRODUCTION

A variety of spatiotemporal patterns, including reaction rate oscillations, are often observed in heterogeneous catalysis systems, such as CO oxidation and NO reduction on platinum surface, etc.[1] At low pressures and typical temperatures, the surface can be regarded as locally well-mixed and simple mean-field models in the form of deterministic reaction-diffusion equations have been very successful to reproduce a lot of experimental observations. However, when looking at very small length scales, internal noises become crucial and must be considered.[2] Internal noises are inherent in chemical reaction systems due to the stochastic nature of the elementary processes including reaction and diffusion, and it is generally accepted that the strength of the internal noise is inversely proportional to the square root of the system size. In heterogeneous catalysis, sufficiently small systems to be strongly influenced by internal noise are provided by the facets of a field emitter tip,[3] by nanostructured composite surfaces,[4] and by the small metal particles of a supported catalyst.[5] Also when the pressures are increased, the size of locally well-mixed cell would decrease to a small scale where a mean-field type of reaction-diffusion equations becomes less accurate and internal noises become important. Therefore, an important question arises: how the internal noises would influence the spatiotemporal dynamics in small heterogeneous catalysis systems?

Only recently has attention been paid to internal noise in heterogeneous catalysis systems. It was found that internal noise can induce transitions between the active and inactive branch of the reaction for catalytic CO oxidation on a Pt field emitter tip.[3] Internal noise becomes essential in the dynamic behavior of CO oxidation when surface cells over low-index single crystal surface are very small.[6] Using a stochastic model,[5,7,8] Peskov and co-workers demonstrated that the large difference between the oscillations observed on a 4-nm and 10-nm Pd particles was a consequence of the interplay between the system's nonlinear dynamics and the internal noise. In the study of spatiotemporal self-organization in catalytic oxidation of hydrogen on Pt(111), the authors also suggested that a mesoscopic stochastic model taking into account internal noise should be used to quantitatively explain the experimental observations.[9] Very recently, experimental study has shown that coverage fluctuations on catalytic particles can drastically alter their macroscopic catalytic behavior, causing bistability to vanish completely with decreasing particle size.[10] The effects of internal noise on pattern formation in nanometer scale, i.e., the nonequilibrium nanostructures, have also been deeply studied.[11]

On the other hand, the constructive roles of noise in nonlinear dynamical systems have attracted great research interest in recent years. It was demonstrated that there exists a "resonant" noise intensity at which the response of the system to a periodic force is maximally ordered, which is well known as stochastic resonance (SR),[12] or the order of the noise-driven system itself can have a maximum in the absence of periodic forcing, which is called coherent resonance (CR).[12] However, most of the studies on SR-like behavior so far only accounts for *ad hoc* external noise, and few attentions have been paid to the constructive roles of internal noise. In previous studies including our work,[13–20] it was found that internal noise can also play SR-like roles in small scale chemical or biochemical reaction systems including intracellular and intercellular calcium signaling, circadian oscillation system, and ion channel gating, which was termed as *internal noise SR* or *internal noise CR*.

In the present paper, we have studied the effect of internal noise on the reaction rate oscillations during the oxidation of CO on low-index platinum surfaces.[6] Here we consider that the surface is divided into small cells inside which the reactant molecules are well mixed, and the reactions inside each cell as well as the exchange of particles between neighboring cells are both stochastic. Therefore, the surface is heterogeneous in a large scale, but homogeneous in small

[a]Author to whom correspondence should be addressed. Electronic mail: hzhlj@ustc.edu.cn

TABLE I. Stochastic processes and reaction rates for CO oxidation on Pt(110). All the parameter values are the same as those listed in Table 2 of Ref. 6.

Process	Rate	Descriptions
$N_{CO}\to N_{CO}+1$	$a_1=NP_{CO}k_{CO}s_{CO}(1-u^{\xi})$	CO adsorption
$N_O\to N_O+2$	$a_2=1/2NP_Ok_O[s_O^{1\times2}(1-w)+s_O^{1\times1}w](1-u)^2(1-v)^2$	O_2 adsorption
$N_{CO}\to N_{CO}-1$	$a_3=N(k_{des}^{1\times2}(1-w)+k_{des}^{1\times1}w)\times u$	CO desorption
$N_{CO}\to N_{CO}-1$ $N_O\to N_O-1$	$a_4=Nk_{re}uv$	Reaction
$N_{1\times1}\to N_{1\times1}+1$	$a_5=Nk_{1\times1}(1-w)\times f_{1\times1}(u,w)$, with $f_{1\times1}(u,w)=(1-\varepsilon)u^{\lambda}+\varepsilon w^{\lambda}$	(1×2) to (1×1)
$N_{1\times1}\to N_{1\times1}-1$	$a_6=Nk_{1\times2}w\times f_{1\times2}(u,w)$, with $f_{1\times2}(u,w)=(1-\varepsilon)(1-u)^{\lambda}+\varepsilon(1-w)^{\lambda}$	(1×1) to (1×2)

scales. Generally, one should develop a stochastic model for the reactions taking place on the whole surface. As the first step, we will focus on the influence of internal noise on the dynamics inside a single cell in the present study and consider the inclusion of diffusion in future works.

For this purpose, we have adopted a recently developed stochastic model[6]and the corresponding chemical Langevin equations.[21] Interestingly, we find that internal noise can play rather nontrivial roles. In a parameter region which is subthreshold for the deterministic oscillatory dynamics, internal noise can induce stochastic oscillations, which are distinct from random fluctuations in that there is a clear peak in the power spectrum. The regularity of the stochastic oscillation, characterized by an effective signal-to-noise ratio (SNR), undergoes two maxima with the variation of the internal noise strength, indicating the occurrence of internal noise coherent biresonance. In addition, we find that the parameter region can be divided into four distinct regions, where the SNR undergoes 2, 1, 0, and 1 maxima, respectively. We show that such a behavior is much relevant to the system's deterministic dynamic features.

II. MODEL AND RESULTS

The model used in the present paper was developed for the oxidation of CO on Pt(110) single crystal surface.[6] The reaction was found to follow a Langmuir–Hinshelwood mechanism, which involves the adsorption of CO or O_2 molecules, and the reaction between adsorbed CO molecules and O atoms. In addition, the adsorbate-induced $1\times1\Leftrightarrow1\times2$ phase transition is taken into account to address the influence of the surface structure on the reactivity. The state of a cell containing N adsorption sites can be described by $\mathrm{X}_N(t)=[N_{CO}(t),N_O(t),N_{1\times1}(t)]^T$, where N_{CO}, N_O, and $N_{1\times1}$ denote the number of adsorbed CO molecules, oxygen atoms, and adsorption sites in a nonreconstructed (1×1) surface, respectively. The system's dynamics is then described by stochastic birth-death processes governed by a chemical master equation, which describes the time evolution of the probability of having a given number of these species. For the present model, the stochastic processes and the corresponding reaction rates are listed in Table I, where we have introduced the concentrations $u=N_{CO}/N$, $v=N_O/N$, and $w=N_{1\times1}/N$. Note that the transition rates $a_{i=1,\ldots,6}$ are all proportional to the system size N.

From these processes, one may readily write down the chemical master equation for this system. However, there is no general procedure to solve this master equation analytically. A well-known method to handle the master equation is the exact simulation algorithm proposed by Gillespie, which mimic the reaction dynamics by randomly determining what the next reaction is and when will it happen.[22] Recently, Gillespie found that under certain circumstances, it is also reasonable to approximate the master equation by a chemical Langevin equation (CLE).[21] In our previous studies,[14–16] we have shown that it is applicable to use the CLE to study the effect of the internal noise in small chemical reaction systems qualitatively. Specifically, given the stochastic processes and transition rates shown Table I, the CLE for the current model reads

$$\begin{aligned}\frac{du}{dt}&=\frac{1}{N}[(a_1-a_3-a_4)+\sqrt{a_1}\eta_1(t)-\sqrt{a_3}\eta_3(t)-\sqrt{a_4}\eta_4(t)],\\ \frac{dv}{dt}&=\frac{1}{N}[(2a_2-a_4)+2\sqrt{a_2}\eta_2(t)-\sqrt{a_4}\eta_4(t)],\\ \frac{dw}{dt}&=\frac{1}{N}[(a_5-a_6)+\sqrt{a_5}\eta_5(t)-\sqrt{a_6}\eta_6(t)],\end{aligned}\tag{1}$$

where $\eta_{i=1,\ldots,6}(t)$ are Gaussian white noises with $\langle\eta_i(t)\rangle=0$ and $\langle\eta_i(t)\eta_j(t')\rangle=\delta_{ij}\delta(t-t')$. The items with $\eta_i(t)$ give the internal noises, which scale as $1/\sqrt{N}$ because $a_{i=1,\ldots,6}\propto N$.

In the macroscopic limit $N\to\infty$, the internal noise items can be ignored and the system's dynamics is described by the deterministic equation,

$$\begin{aligned}&du/dt=(a_1-a_3-a_4)/N,\quad dv/dt=(2a_2-a_4)/N,\\ &dw/dt=(a_5-a_6)/N.\end{aligned}\tag{2}$$

With the variation of the parameters P_O and P_{CO}, the system (2) shows very abundant bifurcation features.[6] In the present paper, we fix $P_O=9.6\times10^{-5}$ mbar, $T=520$ K and choose P_{CO} as the only control parameter. In such a case, the bifurcation diagram of the deterministic system is shown in Fig. 1. There is a supercritical Hopf bifurcation (HB) at $P_{CO}\approx3.557\times10^{-5}$, where a stable limit cycle emerges. The limit cycle disappears via a saddle-node infinite period (SNIPER) bifurcation when it encounters the turning point (TP1) at $P_{CO}\approx3.6151\times10^{-5}$. For P_{CO} less than HB or larger than TP1, the system only shows one stable state, and oscillations

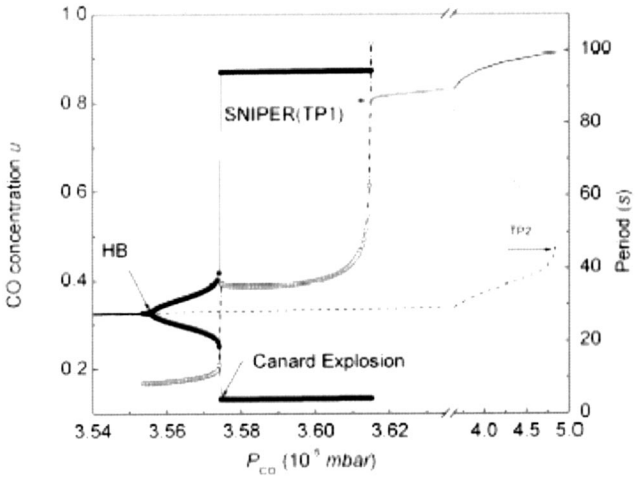

FIG. 1. Bifurcation diagram for the deterministic system (2). HB stands for the supercritical Hopf bifurcation at $P_{CO} \approx 3.557 \times 10^{-5}$, TP1 and TP2 denote two turning points at $P_{CO} \approx 3.6151 \times 10^{-5}$ and $P_{CO} \approx 4.839 \times 10^{-5}$. Stable limit cycles exist in the region between HB and TP1, where the solid circles show the maxima and minima of the oscillations. Note the oscillation ends at TP1 via a saddle-node infinite period (SNIPER) bifurcation. The heavy solid lines denote stable steady states, the dashed line unstable states, and the dotted line saddle states. The dependence of the oscillation period between HB and TP1 is depicted by the open circles (the right axis). Importantly, there is a canard point at $P_{CO} \approx 3.575 \times 10^{-5}$. The bifurcation diagram is calculated by use of the BIFPACK software (Ref. 23).

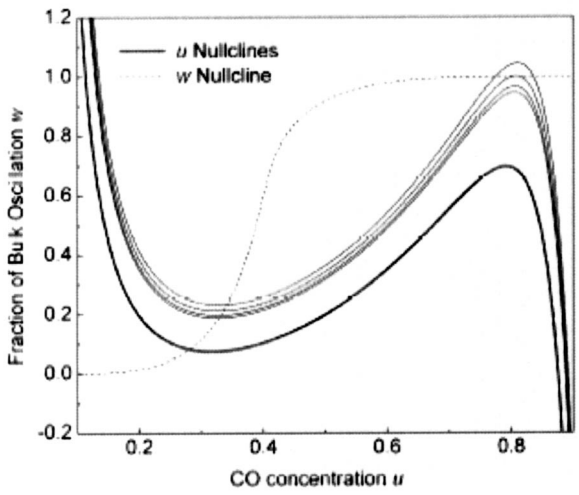

FIG. 2. Nullclines of the deterministic equation (2). Five u nullclines are shown. From bottom to top, $P_{CO} \times 10^5$ are 3.3, 3.56, 3.58, 3.6151, and 3.65 (mbar), respectively. See the text for detailed discussions.

can only be observed in the region between HB and TP1. In addition, an interesting feature of the system is the existence of a canard point (CANARD) at $P_{CO} \approx 3.575 \times 10^{-5}$, where a very fast transition from a small-amplitude oscillation to a large-amplitude oscillation occurs.[24] Therefore, we can divide the bifurcation diagram into four distinct regions, namely, region *A* for $P_{CO} <$ HB, *B* for HB $< P_{CO} <$ CANARD, *C* for CANARD $< P_{CO} <$ SNIPER, and *D* for $P_{CO} >$ SNIPER.

To get more information of the system's deterministic dynamics, we have also drawn the nullclines $\dot{u}=0$ and $\dot{w}=0$ in the *w*-*u* plane for five different parameter values of P_{CO} in Fig. 2. The *w* nullcline does not depend on P_{CO}. The *u* nullcline is S shaped, which contains one minimum and one maximum point. The left branch before the minimum and the right branch after the maximum are both stable and the middle branch in between is unstable. According to Ref. 24, such kinds of manifolds may cause excitability as well as canard phenomenon. From bottom to up, $P_{CO} \times 10^5$ read 3.3, 3.56, 3.58, 3.6151, and 3.65 mbar, respectively. For $P_{CO} = 3.3 \times 10^{-5}$ mbar which is inside region *A*, the two nullclines intersect at one point which is the only stable state. This stable state is also excitable, i.e., small perturbations will cause the system to return immediately to it, while slightly larger perturbations, beyond some well-defined threshold, will cause the system to revert to it only after making a large-amplitude excursion across the right branch of the *u* nullcline. With the increasing P_{CO}, the intersection will move to the middle branch of the *u* nullcline and becomes unstable. When P_{CO} reaches the HB, a small-amplitude limit cycle emerges around the unstable steady state, which will change very fast to a large amplitude limit cycle at a slightly larger value of P_{CO}, the canard point. The *u* nullclines for $P_{CO} = 3.56 \times 10^{-5}$ mbar (in region *B*) and $P_{CO} = 3.56 \times 10^{-5}$ mbar (in region *C*) are shown as examples for these two situations (note that the nullclines do not show much difference when the canard phenomenon occurs). With further increasing of P_{CO}, the right branch of the *u* nullcline begins to intersect with the *w* nullcline, which will create a pair of saddle nodes. At the SNIPER point $P_{CO} = 3.6151 \times 10^{-5}$ mbar, the *w* nullcline is tangent to the *u* nullcline, and the limit cycle ends at a homoclinic orbit with an infinite period. Therefore, the nullclines can help us understand more about the system's dynamics. One will see that such bifurcation features can lead to interesting effects of the internal noise as described below.

To account for the internal noise, we have numerically integrated Eq. (1) using the standard procedure for stochastic differential equations with a time step 0.0l s.[21] To begin, we set the control parameter $P_{CO} = 3.5 \times 10^{-5}$ mbar, which is slightly subthreshold for the deterministic oscillation. Although the deterministic Eq. (2) does not predict self-oscillations for this parameter, the chemical Langevin Eq. (1) can yield stochastic oscillations, which is an important effect of the internal noise. The stochastic oscillation is distinct from random noises in that there is a clear peak in the corresponding power spectrum. Therefore, for reactions in a small surface cell, the rate oscillations may exist in a larger parameter range than that suggested by the deterministic equation. In addition, the dynamic behavior of Eq. (1) shows strong dependence on the cell size *N*, which determines the strength of the internal noise. In Fig. 3, stochastic oscillations for five different cell sizes are shown. For $N = 10^8$, the internal noise is rather small and the system's dynamics approximately obeys the deterministic Eq. (2), hence the CO concentration only shows slight fluctuations around the deterministic steady state as shown in the bottom panel. The corresponding power spectrum density (PSD) of the time series is shown in Fig. 4 (the dashed-dotted-dotted line). There is already a peak in the PSD, implying some "oscillation" information in the time series. When the cell size de-

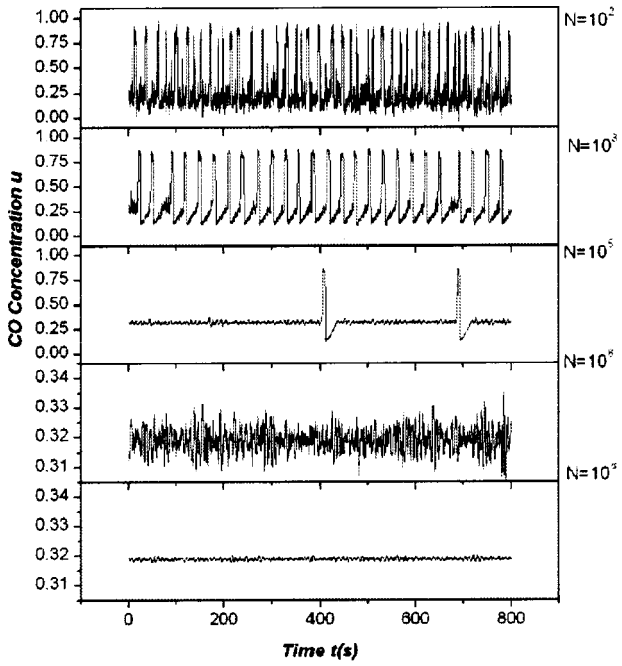

FIG. 3. Stochastic oscillations of CO concentration for different number of adsorption sites N for $P_{CO} \approx 3.5 \times 10^{-5}$ mbar. From top to bottom, N reads 10^2, 10^3, 10^5, 10^6, and 10^8, respectively. Note that the vertical axis has different scales in panels (a)–(c) from those in (d) and (e). For relatively small N, the stochastic oscillations are of large amplitude, while for large N, the amplitude is small. For $N \sim 10^5$, neither type of stochastic oscillations dominates.

creases to a smaller value, e.g., $N=10^6$, random fluctuation around the steady state changes to "stochastic oscillation" of small amplitude, and a clear peak shows in the PSD curve (Fig. 4, dashed-dotted line). With further decreasing of the cell size, we find that occasional random pulses are triggered on the background of the small stochastic oscillations. The hybrid of small oscillations and pulses lead to no peaks in the

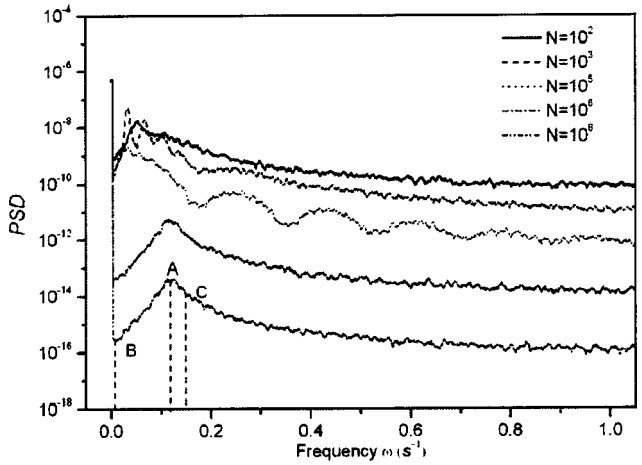

FIG. 4. Power spectrum density (PSD) for the stochastic oscillations shown in Fig. 3. Clear peaks appear except for $N=10^5$. For small N, the peak frequency is smaller, which corresponds to the large-amplitude oscillation. For large N, the peak frequency is larger and the oscillation is of small amplitude. The points A, B, and C in the PSD curve for $V=10^8$ demonstrate how to calculate the effective SNR, i.e., $\mathrm{SNR}=[P(A)/P(B)] \times \omega_A/(\omega_C - \omega_A)$, where $P(\bullet)$ denote the PSD level for a given point and $P(C) = P(A)/e$. Arbitrary unit is used for the PSD. From bottom to top, N reads 10^8, 10^6, 10^5, 10^3, and 10^2, respectively.

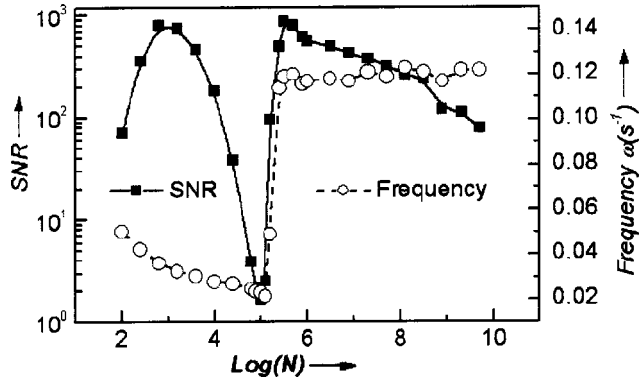

FIG. 5. Dependence of the SNR of the stochastic oscillations on the number of adsorption sites N. Two clear peaks appear, one at $N \sim 10^3$ and the other $N \sim 10^6$. For $N \sim 10^5$, the SNR reaches the lowest level. The corresponding principle frequencies are also shown (right axis). This figure clearly demonstrates the occurrence of internal noise coherent resonance. Since the internal noise level is controlled via the change of N in the present paper, the phenomenon also indicates a kind of system size biresonance.

PSD (Fig. 4, dotted line). For a certain smaller but optimal cell size, $N=10^3$, for instance, the pulses can become rather regular, showing a relatively high and narrow peak in the PSD (Fig. 4, dashed line). If the cell size is too small, the oscillation will be destroyed by the large internal noise, and the peak in the PSD becomes lower and wider again (Fig. 4, solid line). Consequently, with the variation of the cell size N, or correspondingly the internal noise level, small-amplitude stochastic oscillations are first induced and then replaced by the stochastic pulses, the latter becomes the most regular at an optimal system size N, and finally overwhelmed into the internal noise background. For large system size (small internal noise), the stochastic oscillations are of small amplitude, which looks like those deterministic ones in region B (Fig. 1), and for small system size (large internal noise), the system will show large-amplitude stochastic oscillations like those in region C. For both kinds of stochastic oscillations, there seems to be an optimal system size (internal noise level) where the performance of the stochastic oscillation is the best.

To quantitatively characterize the regularity of the stochastic oscillation, we have introduced the effective signal-to-noise ratio (SNR) as already used in our previous studies.[14–16] It is defined as the height of the peak normalized by its relative width, as described in Fig. 4. One may also refer to Refs. 14–16 for more details. The dependence of SNR on system size N is shown in Fig. 5. Two maxima appear, one at $N \sim 10^3$ and the other at $N \sim 10^{5.5}$. Such a behavior may be called system size biresonance, or internal noise coherent biresonance, reminiscent of the great research attention in stochastic resonance and recent interest in system size resonance.[13–20] The corresponding peak frequencies of the stochastic oscillations are also shown in Fig. 5 (right axis). The first maxima ($N<10^5$) corresponds to large-amplitude stochastic oscillations with small frequency, and the second maxima ($N>10^5$) corresponds to small-amplitude stochastic oscillations with large frequency.

The above discussions suggest that it is the specific bifurcation feature shown in Fig. 1 that gives rise to the double

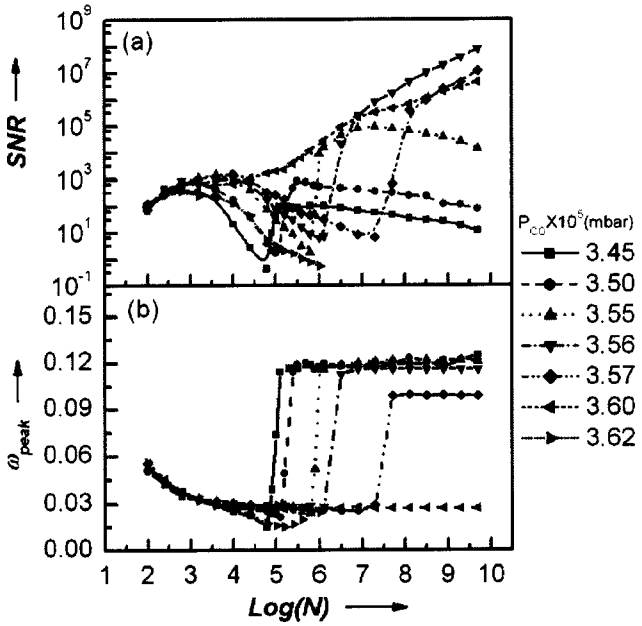

FIG. 6. The dependence of the SNR (a) and frequency (b) of the stochastic oscillations on N for different P_{CO}.

maxima in the SNR$\sim N$ curve. Phenomenologically, when the parameter locates in region A where the system is subthreshold for the deterministic oscillation but excitable, small internal noise tends to draw the system into region B, while large internal noise may cause excitation and drive the system into region C. Therefore, one naturally asks how the behavior depends on the control parameter P_{CO}. To answer this question, we have gone through the parameters from region A to D, and the result is given in Fig. 6. In Fig. 6(a), we find four kinds of dependence on the system size. (a) For parameters in region $A(P_{CO}=3.45\times10^{-5},3.50\times10^{-5},3.55\times10^{-5}$ mbar), there are two maxima, as already described above. (b) For parameters in region $B(P_{CO}=3.56\times10^{-5},3.57\times10^{-5}$ mbar), we also observe a resonance maxima at $N\sim10^3$, which corresponds to the large-amplitude stochastic oscillations. (c) In region $C(P_{CO}=3.60\times10^{-5}$ mbar), the existence of internal noise is destructive. With the increment of internal noise strength, the SNR of the large-amplitude oscillation monotonically reduces. No resonance behavior exists in this range. (d) In region $D(P_{CO}=3.62\times10^{-5}$ mbar), which is also outside the deterministic oscillation region, system size resonance with only one peak occurs again, and the stochastic oscillation is also of large amplitude. The corresponding peak frequencies of the stochastic oscillations are shown in Fig. 6(b), which helps to understand what the stochastic oscillations look like.

Here, it should be pointed out that case (b) is quite distinct to previous understandings. One notes that for parameters in region B, the system already shows deterministic oscillations when internal noise is ignored. In previous studies, it was demonstrated that in such a region, the inclusion of internal noise will only lead to localization and phase diffusion of the original deterministic oscillations, and there is a low limit of system size where the oscillation is no longer correlated in time.[25] Therefore, although it is now widely accepted that internal noise may play constructive roles in the subthreshold region A, the constructive roles of noise in a deterministically oscillation region was not reported before. In our present work, we demonstrate such a possibility in a specific chemical reaction model, which shows peculiar bifurcation features. We think that the existence of a canard explosion from region B to C is the very reason of such a phenomenon. Actually, we have also performed similar studies for other parameter values of P_O. For the deterministic system (2), oscillation only exists for certain range of (P_O,P_{CO}) parameters. We find that if the canard phenomenon disappears then the biresonance behavior in the subthreshold region A cannot happen.

III. DISCUSSION

Using a stochastic model to describe CO oxidation on single crystal platinum surfaces, we have studied the influence of internal noise on the reaction rate oscillations. Considering that the surface is divided into small well-mixed cells, we have focused on the dynamic behavior inside a single cell. In parameter regions where no deterministic oscillations can exist, internal noise can induce reaction rate oscillation, which is in consistent with previous studies in Ref. 6. In addition, we find that the regularity of the stochastic rate oscillations can show two maxima with the variation of the internal noise level, which is changed via the variation of the cell size N, one at $N\sim10^3$ and the other at $N\sim10^{5.5}$. The relationship between such a phenomenon of internal noise stochastic biresonance with the deterministic bifurcation features of the system is also discussed.

As stated in the Introduction, in most experiments, the system's dynamics can be well described by reaction-diffusion models. Usually, external parameter fluctuations as well as surface heterogeneity are more important factors than the internal noise. Therefore, how the results of the present study, which accounts for the interesting role of internal noise in a single cell, would be relevant to real systems is an open question. At the current stage, a few points may be addressed. First, the occurrence of noise induced oscillation and stochastic resonance indicates that internal noise can play some nontrivial, constructive roles in the dynamics of heterogeneous catalysis. Furthermore, because of the existence of two maxima, we find that internal noise might also be crucial for a relatively large cell containing surface sites up to $N\sim10^6$. We note that this is different from previous studies such as in Ref. 6, where it was stated that internal noise may become crucial only when the cell size N is less than 10^4. (Note the first maxima $N\sim10^3$ in the present work coincides with this statement.) The reason may be that the second maximum corresponds to small-amplitude oscillation here and we have tuned the parameter P_{CO} in the very vicinity of the Hopf bifurcation. Finally, present work acts as the preceding step to study the effects of internal noise on the spatiotemporal dynamics on the larger scale surface in future works, especially when the system lies close to some critical points.

ACKNOWLEDGMENTS

This work was supported by the National Science Foundation of China (Grant Nos. 20203017 and 20433050) and the Foundation for the Author of National Excellent Doctoral Dissertation of People's Republic of China (FANEDD).

[1] R. Imbihl and G. Ertl, Chem. Rev. (Washington, D.C.) **95**, 697 (1995); M. Eiswirth and H. H. Rotermund, Physica D **84**, 40 (1995); M. Bär, E. Meron, and C. Utzny, Chaos **12**, 204 (2002).
[2] N. G. van Kapman, *Stochastic Processes in Physics and Chemistry* (North-Holland, Amsterdam, 1987); W. Horsthemke and R. Lefever, *Noise-Induced Transitions* (Springer, Berlin, 1984).
[3] Y. Suchorski, J. Beben, E. W. James, J. W. Evans, and R. Imbihl, Phys. Rev. Lett. **82**, 1907 (1999).
[4] A. T. Bell, Science **299**, 1688 (2003).
[5] N. V. Peskov, M. M. Slinko, and N. I. Jaeger, J. Chem. Phys. **116**, 2098 (2002).
[6] C. Reichert, J. Starke, and M. Eiswirth, J. Chem. Phys. **115**, 4829 (2001).
[7] N. I. Jaeger, N. V. Peskov, and M. M. Slinko, React. Kinet. Catal. Lett. **44**, 183 (2003).
[8] N. V. Peskov, M. M. Slinko, and N. I. Jaeger, Chem. Eng. Sci. **58**, 4797 (2003).
[9] C. Sachs, M. Hildebrand, S. Volkening, J. Wintterlin, and G. Ertl, Science **293**, 1635 (2001).
[10] V. Johanek, M. Laurin, A. W. Grant, B. Kasemo, C. R. Henry, and J. Libuda, Science **304**, 1639 (2004).
[11] M. Hildebrand and A. S. Mikhailov, J. Phys. Chem. **100**, 19089 (1996); M. Hildebrand, A. S. Mikhailov, and G. Ertl, Phys. Rev. Lett. **81**, 2602 (1998); M. Hildebrand and A. S. Mikhailov, J. Stat. Phys. **101**, 599 (2000).
[12] L. Gammaitoni, P. Hänggi, P. Jung, and F. Marchesoni, Rev. Mod. Phys. **70**, 223 (1998); P. Hänggi, ChemPhysChem **3**, 285 (2002).
[13] G. Hu, T. Ditzinger, C. Z. Ning, and H. Haken, Phys. Rev. Lett. **71**, 807 (1993); A. Pikovsky and J. Kurths, *ibid.* **78**, 775 (1997).
[14] Z. H. Hou and H. W. Xin, ChemPhysChem **5**, 407 (2004).
[15] J. Zhang, Z. H. Hou, and H. W. Xin, ChemPhysChem **5**, 1041 (2004).
[16] Z. H. Hou and H. W. Xin, J. Chem. Phys. **119**, 11508 (2003).
[17] P. Jung and J. W. Shai, Europhys. Lett. **56**, 29 (2001).
[18] G. Schimid, I. Goychuk, and P. Hänggi, Europhys. Lett. **56**, 22 (2001).
[19] J. W Shuai and P. Jung, Phys. Rev. Lett. **88**, 068102-1 (2002).
[20] J. W. Shuai and P. Jung, Biophys. J. **83**, 87 (2002).
[21] D. T. Gillespie, J. Chem. Phys. **113**, 297 (2000); *Handbook of Stochastic Methods for Physics, Chemistry, and the Natural Science*, edited by C. W. Gardiner (Springer-Berlin, 1983).
[22] D. T. Gillespie, J. Phys. Chem. **81**, 2340 (1977).
[23] *Pratical Bifurcation and Stability Analysis: From equilibrium to Chaos*, 2nd ed., edited by R. Seydel (Spinger-Berlin, 1999), free software on website http://www.bifurcation.de/software.html
[24] M. Brøns and K. Bar-Eli, J. Phys. Chem. **95**, 8706 (1991); M. Krupa and P. Szmolyan, J. Diff. Eqns. **174**, 312 (2001); H. G. Rotstein, N. Korpell, A. M. Zhabotinsky, and I. R. Epstein, J. Chem. Phys. **119**, 8824 (2003); SIAM J. Appl. Math. **63**, 1998 (2003).
[25] P. Gaspard, J. Chem. Phys. **117**, 8905 (2002); D. Gonze, J. Halloy, and P. Gaspard, *ibid.* **116**, 10997 (2002).